

LNF-73/26  
4 Giugno 1973

W. W. Ash, P. Monacelli, M. Piccolo and F. Ronga:  
PERFORMANCE OF CYLINDRICAL WIDE GAP SPARK  
CHAMBERS WITH TRANSPARENT WIRE ELECTRODES.

W. W. Ash<sup>(x)</sup>, P. Monacelli<sup>(o)</sup>, M. Piccolo and F. Ronga: PERFORMAN-  
CE OF CYLINDRICAL WIDE GAP SPARK CHAMBERS WITH TRAN-  
SPARENT WIRE ELECTRODES. -

1. - INTRODUCTION. -

Two large wide-gap spark chambers with transparent wire electrodes will be used for the measurements of the outgoing particle momenta in the magnetic spectrometer experiment (MEA) at Adone. The chambers have four gaps each with cylindrical electrodes and cannot be viewed in the usual way, that is through the plexiglass frames because of the presence of iron in the magnetic flux return.

The magnet is a 2 meters long solenoid with a diameter of 2 meters and axis perpendicular to the electron positron beams. The use of wire electrodes instead of the usual aluminium foils, reduces the multiple coulomb scattering and more importantly allows one to view the sparks through the transparent electrodes themselves. In this way the complete spacial reconstruction is made possible even using only one view (see Fig. 1)<sup>(1)</sup>.

For the construction and the search of good working conditions of these chambers, with about 2 m<sup>3</sup> of sensitive volume, we had

---

(x) - Now at Stanford Linear Accelerator Center U.S.A.

(o) - Istituto di Fisica dell'Università - Roma and Istituto Nazionale di Fisica Nucleare Sezione di Roma, Italy.

2.

to overcome many difficulties due to the great dimensions, to interference problems between the gaps and to the effects caused by the distortion of the electric field at the edges.

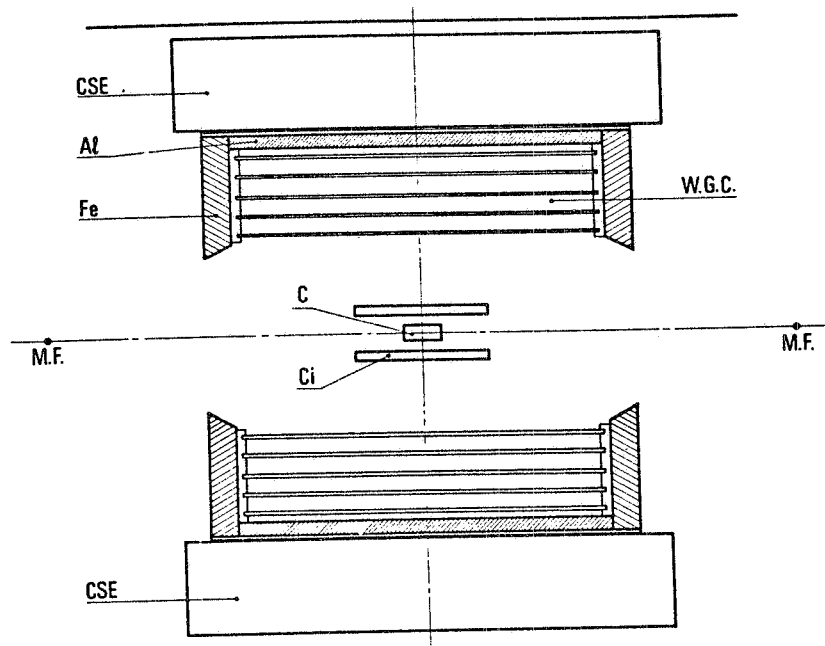


FIG. 1 - Experimental lay out of the MEA experiment.  
CSE: External spark chambers; Al: Aluminium bobbin  
Fe: Iron for magnetic flux return; C: Vacuum pipe of  
Adone; Ci: Internal narrow-gap spark chambers;  
MF: Cameras; WGC: Internal cylindrical wide gap spark  
chambers.

In this note we shall briefly describe the solution to these problems obtained at first using some small dimension prototypes and then the final chambers; also we shall report the precision one can achieve in the momentum reconstruction using these chambers.

## 2. - TESTING THE PROTOTYPES. -

At first a monogap with plane wire electrodes (dimension  $30 \times 10 \times 10 \text{ cm}^3$ ) was tested and a rather surprising effect was observed: the chamber efficiency depended strongly on the distance between H. V. plane and one of the scintillator counters used for triggering the chamber. In addition we did not succeed in obtaining high efficiencies with a bigap chamber having internal electrodes consisting of single-layer of wires; we ascribed those two effects to the same origin, of electrostatic nature, and decided to investigate more accurately this problem.

A second chamber was built similar to the first one, but with one of the electrodes ( $P_{bc}$ ) made by two layers of wires (0.1 mm in diameter and 2,5 mm spaced) with an intergap distance of 1.5 cm (see Fig. 2). The second electrode ( $P_a$ ) was made of an easily changeable plane so that we were able to test wires with different diameters and different spacings.

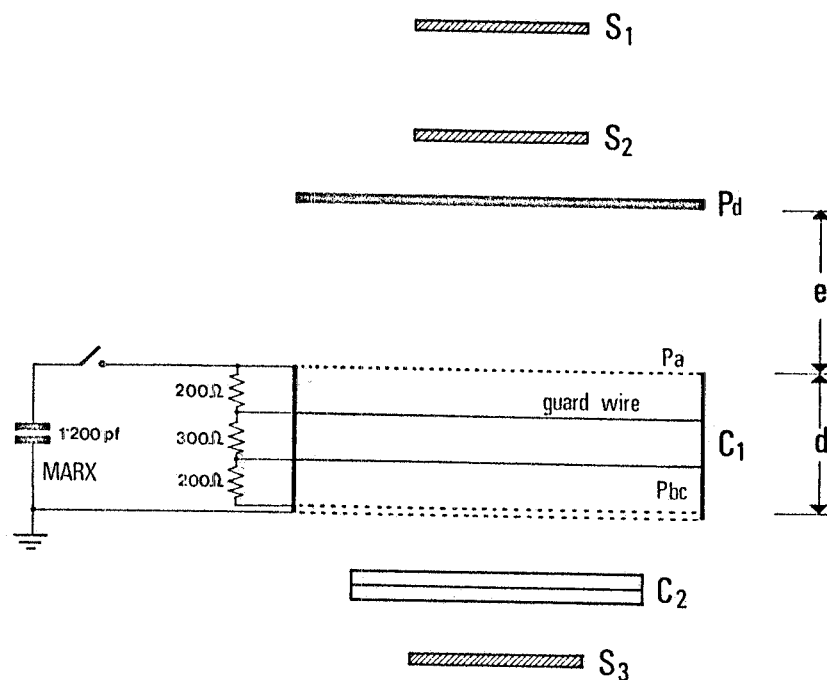


FIG. 2 - Experimental set up of the wide gap prototype for testing the efficiency as a function of the distance  $e$  of the aluminium foil  $P_d$  for various wire configurations.

The chamber was fired using a four stage pressurized Marx generator with an output capacitance of 1200 pf, triggered by a scintillation counter telescope on cosmic rays ( $S_1, S_2, S_3$ ). The efficiency was measured for different experimental configurations as a function of the distance  $e$  between the high voltage electrode and the aluminium foil  $P_d$  ( $30 \times 30 \text{ cm}^2$ ) at ground potential.

In Fig. 3 the efficiency is shown as a function of  $1 + d/e$  where  $d$  is the gap spacing;  $1 + d/e$  is proportional to the electric charge (and therefore to the maximum field) on a wire of the intermediate layer  $P_a$ . As one can see the efficiency shows a rather sharp knee corresponding to  $e = 11 \text{ cm}$  if  $P_a$  is made with  $100 \mu$  wires, 2,5 mm spacing (Fig. 3a). The position of the knee is not very sensitive to the diameter of the wires of  $P_a$  (from 100 to  $200 \mu$ ) or the spacing (from 2,5 to 1,25 mm) (Fig. 3b, 3g).

4.

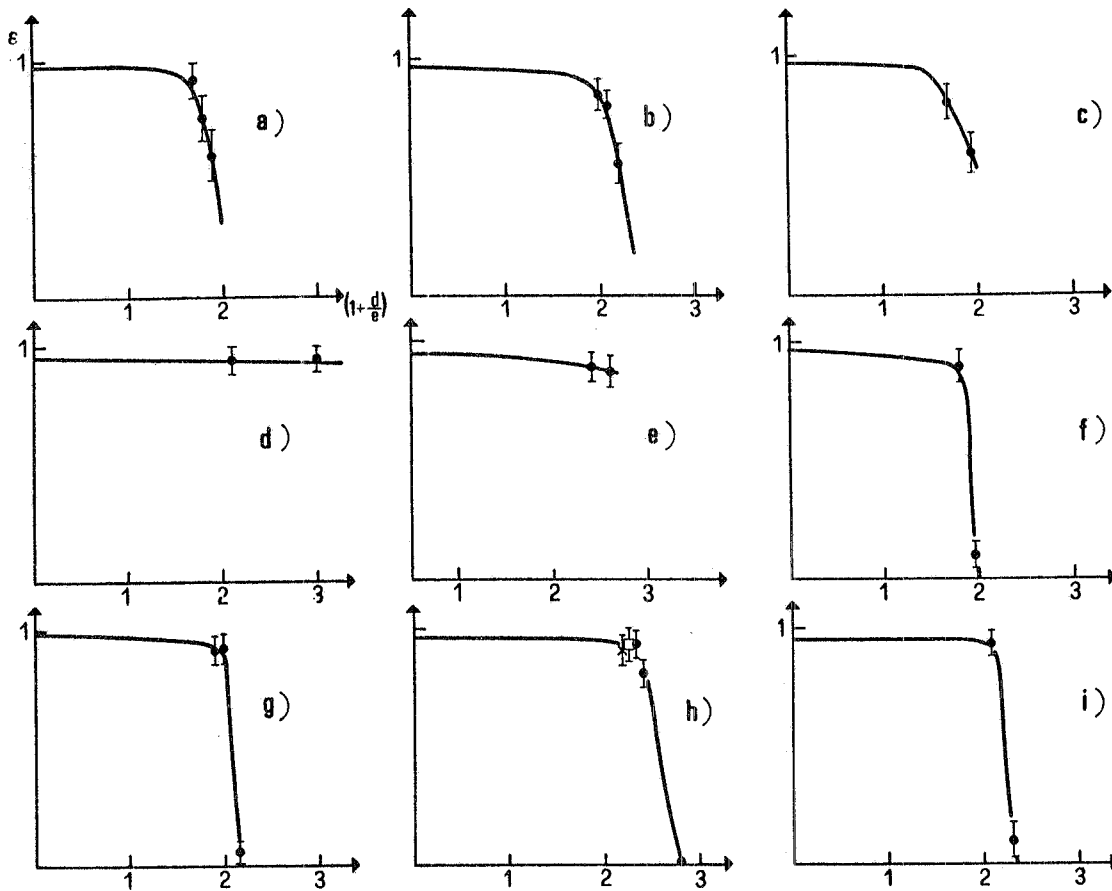


FIG. 3 - Plots of the efficiency as a function of  $1+d/e$ .

- a) 0.1 mm wires 2.5 mm spacing  $E = +4.4$  KV/cm, (30% neon, 70% helium)
- b) 0.2 mm wires 2.5 mm spacing  $E = +4.4$  KV/cm, (30% neon, 70% helium)
- c) 0.2 mm wires 2.5 mm spacing  $E = -4.4$  KV/cm (30% neon, 70% helium)
- d) 0.2 mm wires 2.5 mm spacing  $E = +7$ .KV/cm (30% neon, 70% helium +  $H_2O$  at vapour pressure)
- e) 0.2 mm wires 2.5 mm spacing  $E = +4.4$  KV/cm (80% neon, 20% helium)
- f) 0.2 mm wires 2.5 mm spacing  $E = -4.4$  KV/cm (80% neon, 20% helium)
- g) 0.1 mm wires 1.25 mm spacing  $E = +4.4$  KV/cm (30% neon, 70% helium)

In the next two diagrams h, i,  $P_d$  is near the double wire planes  $P_{bc}$  now at H. V.

- h) 0.1 mm 2.5 mm  $E = 4.4$  KV/cm (30% neon, 70% helium)  
 $E = 6$  KV/cm  
 $E = 8$  KV/cm
- i) The same as before only  $E = -4.4$  KV/cm

The growth of the electric field near the wires of  $P_a$  when  $P_d$  approaches does not explain this effect completely because the efficiency of the chamber with  $P_d$  at infinity remained in plateau up to the maximum field (8 KV/cm) which we could reach with our Marx generator. Therefore one can conclude that it is the different shape of the electric field near the wires that plays an important role in this effect (see Fig. 4-5).

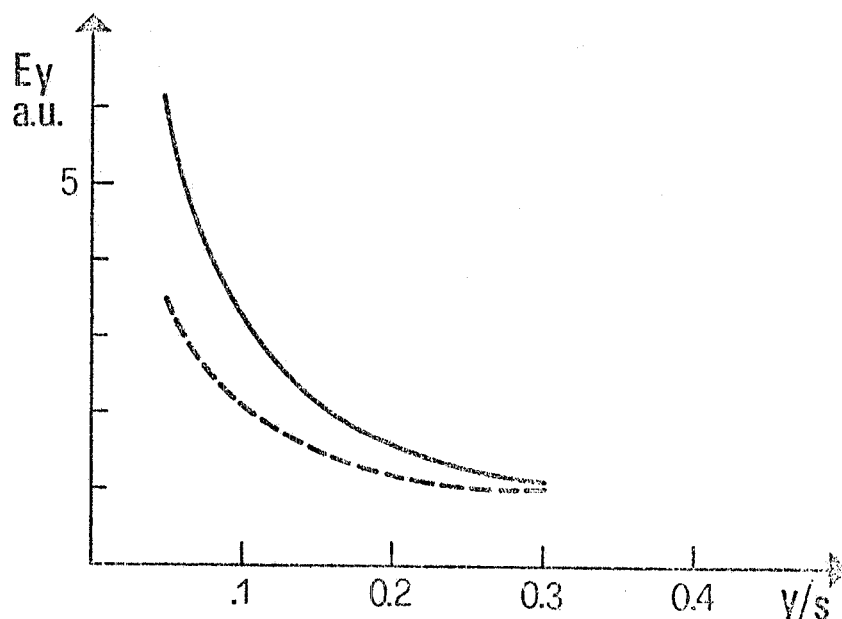


FIG. 4 - Behaviour of electric field along a line perpendicular to the plane of wires and intersecting a wire as a function of the distance from the wire in units of wire spacings. ---- for the middle plane of a bigap; ——— in the case of a monogap.

Some improvement can be obtained increasing the percentage of neon in the gas mixture (see Fig. 3e); the improvement is bigger if one adds water vapour at vapour pressure at  $20^{\circ}$  (see Fig. 3d). If the sign of the electric field ( $P_a$  wires negative) is changed one observes a lower efficiency; this effect is due to the well known change of breakdown potential between a wire and a plane, if one changes polarity<sup>(2, 3)</sup>.

In Figure 3h, i we report some measurements made moving  $P_d$  near the double plane  $P_{b,c}$ , with  $P_{b,c}$  now at high voltage. One can see a net improvement both for positive and negative pulse

6.

polarity, and the efficiency remains good up to  $E \approx 8 \text{ KV/cm}$ .

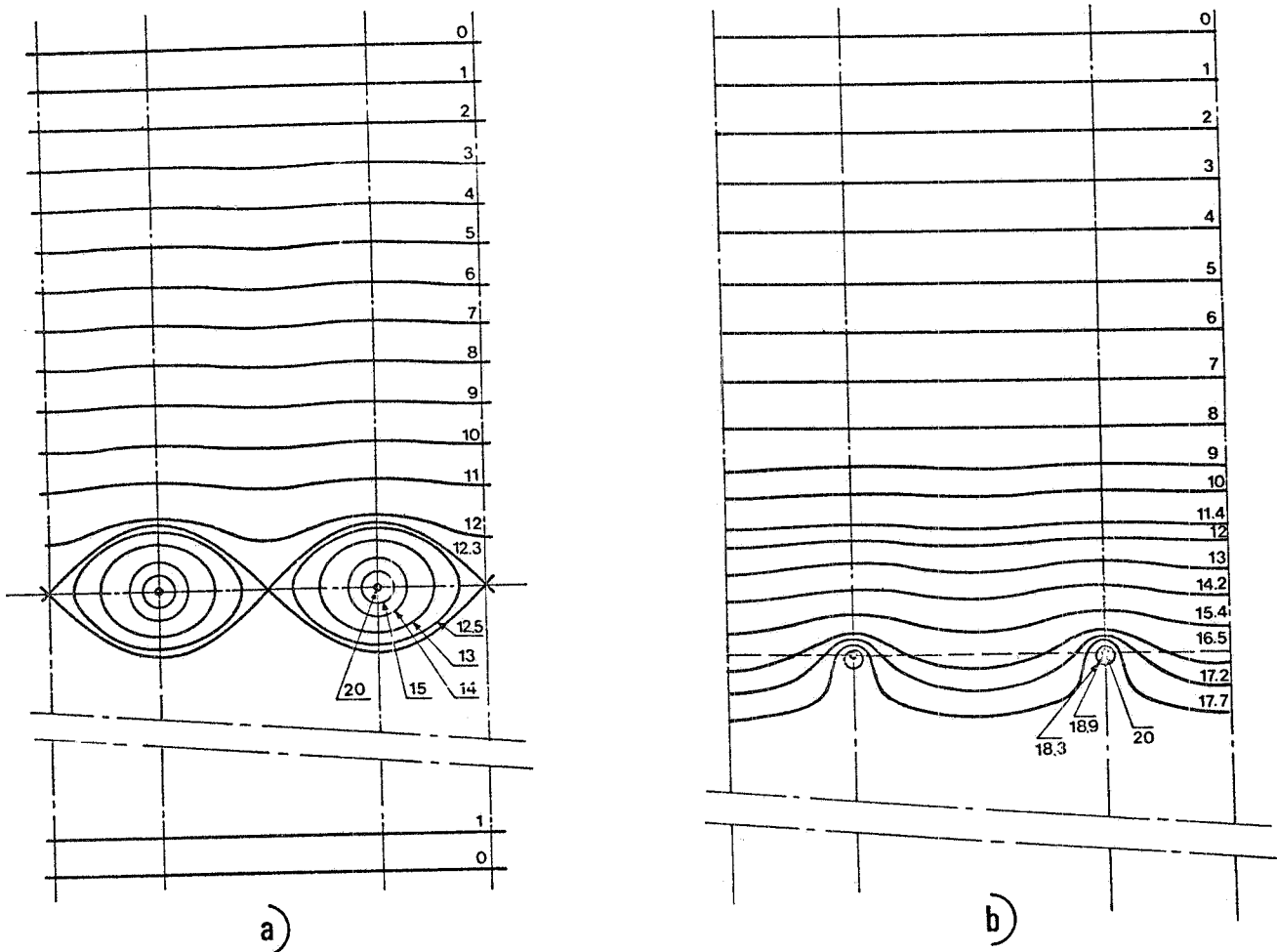


FIG. 5.- Equipotential lines near the wires in the case of a bigap (a) and in the case of a monogap (b).

In conclusion we can say that all these tests show that it is quite difficult to get wide multigap chambers with wire electrodes working well without adding quenching agents or without doubling all the internal electrodes. We adopted this last solution in order to be sure that also the larger chamber would work well.

### 3. - THE LARGE-CHAMBERS. -

The chambers built for the MEA experiment are four gap cylindrical chambers with  $r=1 \text{ m}$  for the external electrode and  $r \approx 50 \text{ cm}$  for the most internal electrode. The length is  $\approx 2 \text{ m}$  and the angular opening of the cylindrical sector is  $120^\circ$  (see Fig. 6).

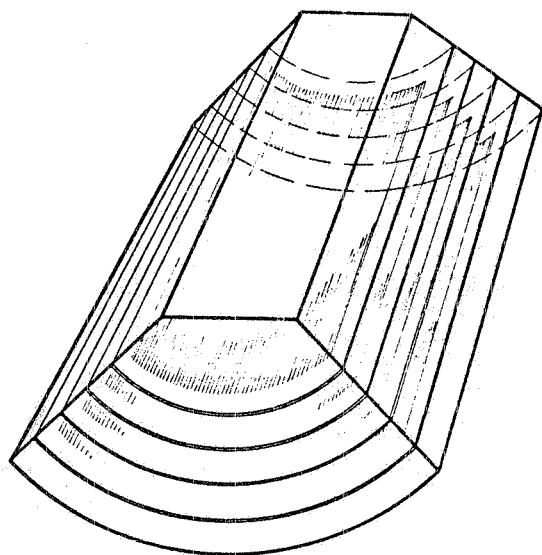


FIG. 6 - One of the two wide gap cylindrical spark chambers with wire electrodes to be used in the MEA experiment.

As a consequence of the measurements reported in the preceding section each wire electrode was made with two layers of wires 2.5 cm apart. The diameter of the wires is  $100\mu$  and the spacing 2.5 mm. The double wire electrodes also make the spatial reconstruction easier, since some parts of the chambers are seen by only one photographic camera and the spatial reconstruction of the tracks in these zones is possible only for the points at the beginning and at the end of the spark, where the track crosses the cylindrical surfaces defined by these electrodes. If the electrodes are double the track is seen as four separated segments and the beginning and the end of each spark is easily recognised. Unfortunately, it is also true that the end points of the spark are the points with biggest distortion. We shall discuss this problem in the next section.

The dimension of the chambers are such that for very rapid signals one can observe delay-line effects, the characteristic impedance is of the order of  $40\ \Omega$ . The rise time of the applied H.V. pulse is about 50 ns, much longer than the transmission time of the chambers; one can therefore also work without adapting the chamber. Nevertheless as is known<sup>(4)</sup>, a low resistance  $R$  in parallel to the chamber together with a high output capacity  $C$  of the Marx generator improves the efficiency for multiple tracks compared to a configuration with high resistance and low output capacity. However for obvious reasons one also has to limit the instantaneous current in the wires thus setting an upper value to  $C$  for fixed  $R$ .

As we noted already in the prototypes with plane electrodes, also for the big cylindrical chamber a large number of guard wires were necessary in order to achieve good working conditions. We had 15 guard wires for each gap connected through a resistor chain to the



8.

ground and HV electrodes so that the electric field near the edges was almost equal to the field inside the gaps when the HV pulse was applied to the chamber. The chain was made of 14 resistor of  $33\ \Omega$  each. Without wires or with an insufficient number of them we noticed many spurious sparks near the edges with consequent loss of efficiency; this effect became bigger with a metal plane at earth potential near the edges. It was also necessary to put a metal strip  $\sim 2.5$  cm large along the frames at the edge of the double layers of wires. The gas mixture used was neogal 90 ( $\sim 90\%$  neon and  $\sim 10\%$  helium) in order to be able to work with good efficiency even with rather low electric fields. The efficiency dependend strongly on the gas purity in the chamber and we decided to recover the neogal after one pass through the chamber; the recovered gas was recompressed and purified by the cryogenic group of the Frascati National Laboratories (a system of activate charcoal traps at liquid nitrogen temperature, was used). This recovery had the advantage, with respect to continuous purification systems, of a greater "local" semplicity and a less maintenance; in fact the gas was purified only from time to time when a certain number of cylinders were filled. We also added to the gas about 10% alcohol at room temperature vapour pressure in order to minimize spurious sparks. The applied HV pulse was generated by a 3 stages Marx with 6.600 pf output capacity. The total shunt resistance applied in parallel to the chamber was  $25\ \Omega$ . The efficiency for small angle tracks is about 100% per gap for electric fields of the order of 6 KV/cm. This efficiency remains nearly constant up to angles (with respect to the electric field) of  $\sim 40^\circ$ , for greater angles the sparks become less bright and eventually vanish. As one can see, the geometry of the chamber is such that for straight tracks the sparks make angles with the electric fields which are bigger in the inner electrodes than in the more external ones. Therefore very inclined tracks may have no visible sparks in the most internal gaps. Figure 7 shows a typical cosmic ray event.

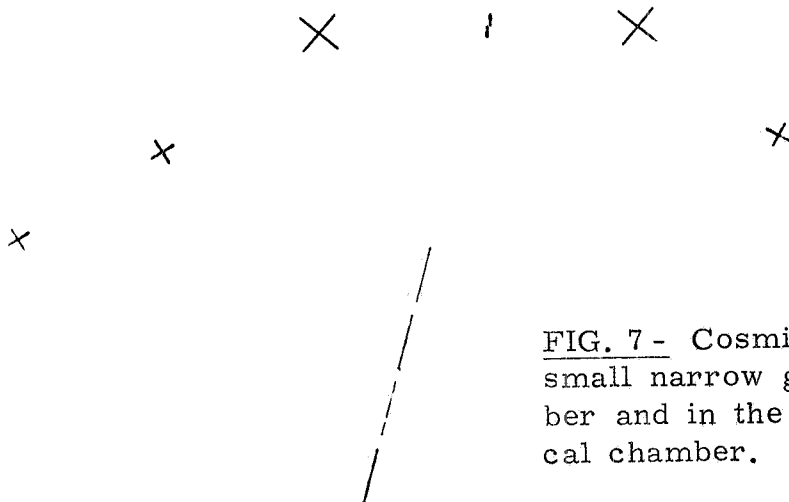


FIG. 7- Cosmic ray event in a small narrow gap reference chamber and in the wide gap cylindrical chamber.

## 4. - PRECISIONS DETERMINATION. -

As is already known in wide gap spark chambers there is a systematic error due to the coherent shift of the electrons along the applied electric field. This shift depends on the gas type and on the form and amplitude of the high voltage pulse, and adds to the errors due to incoherent distortion of the tracks<sup>(5, 6)</sup>. In the presence of a magnetic field  $\vec{B}$  there will also be some displacement in the direction  $\vec{E} \wedge \vec{B}$ .

These coherent shifts of the sparks can give a systematic error to the curvature of the trajectory of the particle; this is particularly true in a configuration such as ours with four cylindrical gaps. In fact the corrections one has to make are different for each of the four gaps because the trajectory of the particle will generally define a different angle with respect to the electric field in the various gap. The shift of the sparks due to the electric field has been measured with cosmic rays without magnetic field as a function of the angle between spark and electric field.

The distance of the sparks from a straight line fit of all the measured points was computed. (The points used in the fit were four points in a narrow gap reference chamber and six points along the spark of each wide gap excluding the extreme points of each spark). This fitted trajectory represents only the first approximation of the real trajectory of the ionizing particle because of the presence of the shifts which are different in the 4 gaps. Therefore we preferred to use the differences between fit deviations in successive gaps ( $d_i - d_{i+1}$ ). The effective shift of the track along the electric field is related to this difference by the relation

$$(1) \quad D = \frac{d_i - d_{i+1}}{2 \sin \theta}$$

where  $\theta$  is the mean angle of the two tracks respect to the electric field.

The pictures taken have been measured on a scanning table with a total demagnification factor 2 compared with the real dimensions. In these measurements we had a total scanning error for each point of the order of  $200 \mu$  in the real space (this error contains also the incoherent distortion of the spark which gives a contribution less than  $100 \mu$ <sup>(6)</sup>). The distribution of the mean angles of the tracks with the electric field in the first gap is shown in Fig. 8a.

In Fig. 8b we report the distribution of the displacement D

10.

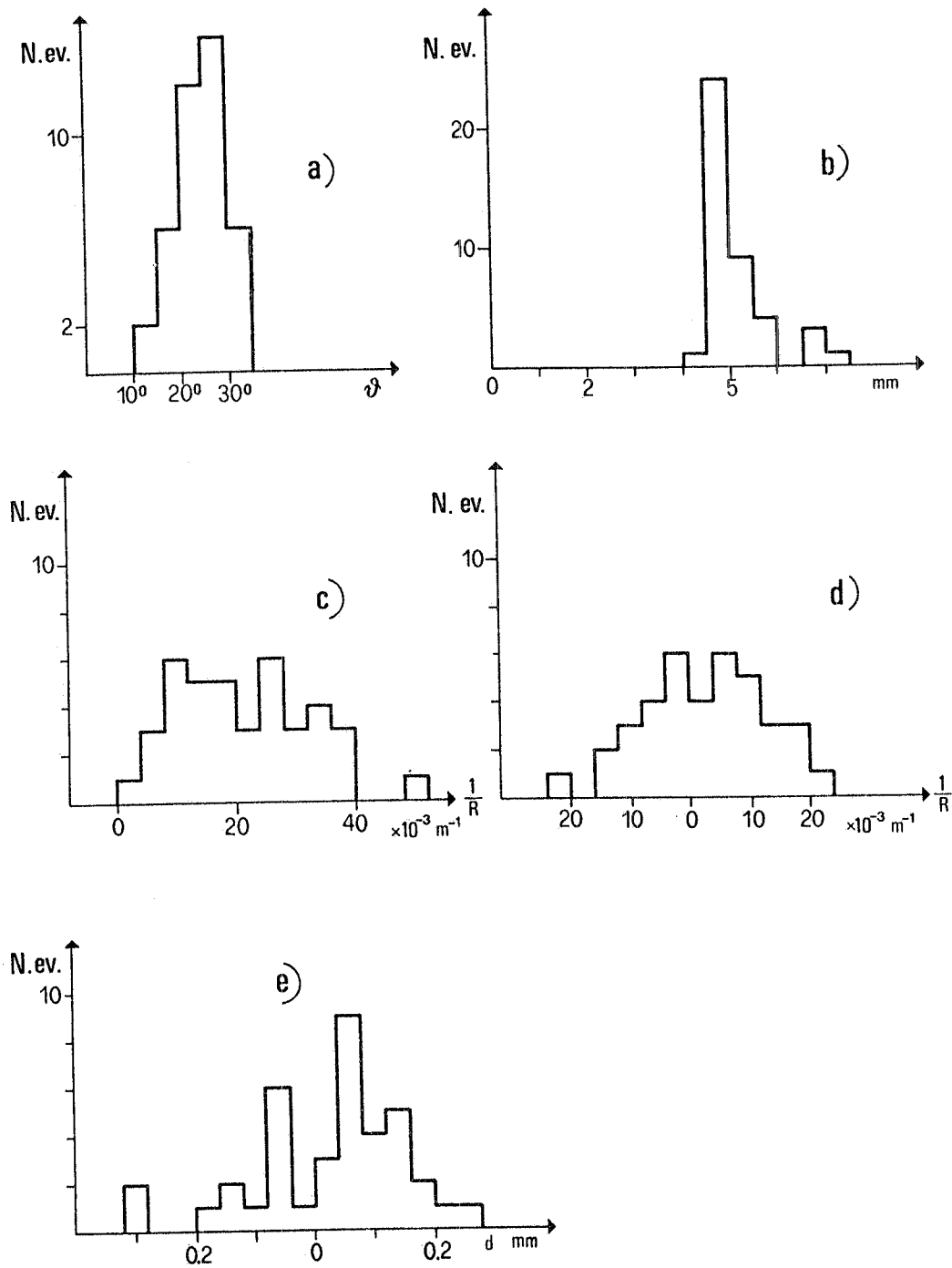


FIG. 8 - a) Distribution of mean angles  $\theta$  of the tracks with the electric field in the first gap; b) Distribution of the displacement  $D = d_1 - d_2 / 2 \sin \theta$  of the same events of figure 8a, where  $d_1$  and  $d_2$  are the distances of the spark in the first and second gap from the fitted trajectory; c) Distribution of curvatures; d) Distribution of curvatures after the correction of the drifts; e) Distribution of the distance of the first spark after the correction of the shifts.

defined from relation (1) for the first two gaps; the other two pairs of gaps have similar distributions. The fact that the distributions are narrow demonstrates that  $D$  is practically independent of the angle. The value of  $D$  which one gets from these distributions is  $D \approx 5$  mm. In Fig. 8c we report the distributions of the apparent curvature of the measured tracks, obtained with a quadratic fit of the four tracks. The distribution is not centered about zero, owing to the above mentioned shifts and to the fact that the counter telescope selected only events inclined in same direction. A first approximation correction has been done assuming  $D = 5$  mm constant for the 4 gaps; in this way we obtained a better approximation for the effective trajectory of the particle (linear fit of all the corrected points) and we calculated the new shifts  $D$  for every gap with respect to this new line. The values obtained in this way were  $D = 5.0$  mm for the three most internal gaps and  $D = 4.5$  mm for the most external gap. The difference is due to the fact one of the electrodes of the last gap is an aluminium plate and not a wire plane so that the discharge times are shorter. In Fig. 8e the distances  $d_1-d_2$  of the first two gaps are shown after these corrections have been made; one notices that the distribution is centered about zero and that the half-width is compatible with the total scanning error. One also gets better curvature distributions (Fig. 8d) with a mean value is of  $\sim 1.7 \cdot 10^{-3} \text{ m}^{-1}$  and a half width of  $\sim 9 \cdot 10^{-3} \text{ m}^{-1}$ . This results are quite similar to those reported in ref. (7), obtained with a monogap of 40 cm.

In all these measurements the extreme points of the tracks have not been considered because the track does not have the same behaviour near the electrodes as it does in the central zone. This effect has been measured and has shown to be quite large near the negative electrode (see Fig. 9a). Shifting laterally the end point

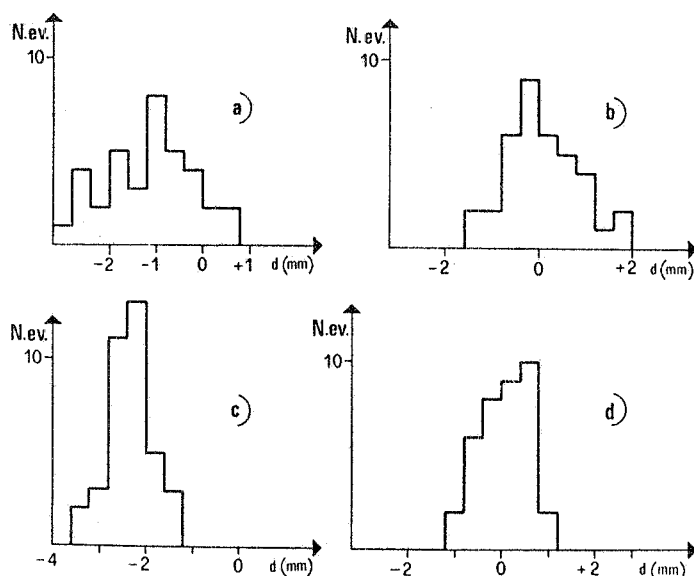


FIG. 9 - a) Distribution of the distances of the fitted trajectory from the points of the spark near to the negative electrode of the first gap; b) the same as in a) but after correction reported in the text. c) Distribution of the distance of the fitted trajectory from the points of the spark near to the positive electrode in the first gap; d) The same as in c) but after the correction reported in the text.

of the track through a distance given by  $A \sin^2 \theta$  with  $A = 6$  mm, one is able to correct this error quite well (see Fig. 9b). The endpoint of the track near the positive electrode behaves a little better (see Fig. 9c) and can be corrected with a shift of  $A \sin \theta$  with  $A = 6$  mm for the first 3 gaps and  $A = 5$  mm for the last gap (see Fig. 9d).

#### ACKNOWLEDGMENTS. -

All the members of the MEA group have (in one way or another) contributed to this work and their suggestions and help is gratefully acknowledged.

Most of the credit for the good performance of the chambers goes to the staff of the Frascati High Energy Mechanical shop directed by Mr. G. Di Stefano where many different problems were resolved in a skillful manner. Thanks are due to the Frascati Cryogenic Group for the recovery and purifications systems of the gas used in the chambers. Thanks are also due to G. Schina for his constant technical assistance and to P. Sartori for scanning and data handling.

#### REFERENCES. -

- (1) - W. W. Ash et al., A magnetic analyzer to be used for Adone colliding beam experiments, Frascati report LNF-69/2.
- (2) - Popoular, "Electrical phenomena in gases", pag. 163.
- (3) - F. Llewellyn-Jones, Ionization and breakdown in gases (Methuen monograph, London, 1957).
- (4) - A. E. Brenner et al., Observations on the performance of wide-gap spark chambers, Nuclear Instr. and Meth. 103, (1972).
- (5) - W. W. Ash and D. Bisello, Report INFN/TC-70/2 (1970).
- (6) - D. Bisello and F. Ronga, Frascati Report LNF-70/44 (1970).
- (7) - Garron, Grossman and Strauch, Properties of wide-gap spark-chambers, Rev. Sci. Instr. 36, 264 (1964).